Proceedings of the International Symposium on Mathematical Methods in Engineering

Editors
Kenan Taş
Dumitru Baleanu
J.A.Tenreiro Machado

27-29 April 2006
Çankaya University
Ankara, Turkey

ÇANKAYA ÜNİVERSİTESİ
1997

Co-Sponsored by TÜBİTAK
TÜBİTAK

Analysis of Fractional-Order Discrete Controllers in the Presence of Nonlinearities

Ramiro S. Barbosa, J. A. Tenreiro Machado, and Alexandra M. Galhano

Institute of Engineering of Porto,
Polytechnic Institute of Porto, Porto, Portugal
`{rsb,jtm,amf}@isep.ipp.pt`

Abstract *— Presently, the development of fractional-order controllers is one of the most promising fields of research. However, most of the work in this area addresses the case of linear systems. In this paper we consider the analysis of fractional-order control of nonlinear systems. The performance of discrete fractional-order controllers in the presence of several nonlinearities is discussed. Some results are provided that assesses the superior robustness of such algorithms.*

1 Introduction

The concepts involved with fractional calculus (FC) theory – the area of mathematics that handles the derivatives and integrals to an arbitrary order (real or complex order) – are, nowadays, applied in almost all the areas of science and engineering, being recognized its ability to yield a superior modelling and control in many dynamical systems [1–3].

In what concerns the area of control systems, we can report only a few works that addresses the study of fractional-order systems in the presence of nonlinear phenomena [4–6]. Nevertheless, it is common to find different types of nonlinearities in real systems (such as the saturation at the actuator or the backlash in gear systems). Therefore, the analysis and performance of the fractional-order controllers under their presence is of great practical interest.

Nowadays, the widespread use of the fractional-order controllers has been justified by its superior performance over the classical control techniques, particularly when used for the control of fractional-order systems. One example is the generalization of the well-known PID controller by introducing an integrator of order $0 < \lambda \leq 1$ and a differentiator of order $0 < \mu \leq 1$ (where the orders λ and μ may assume real noninteger values). The transfer function of such a $PI^\lambda D^\mu$-controller is given by:

$$C(s) = K_p \left(1 + \frac{1}{T_i s^\lambda} + T_d s^\mu \right)$$

(1)

where λ and μ are positive real numbers; K_p, T_i and T_d are correspondingly the proportional gain, the integral time constant and the derivative time constant. Clearly, taking

$(\lambda, \mu) = \{(1, 1), (1, 0), (0, 1), (0, 0)\}$ we get the classical $\{$PID, PI, PD, P$\}$-controllers, respectively. Moreover, the $PI^\lambda D^\mu$-controller is more flexible and gives the possibility of adjusting more carefully the dynamical properties of a fractional-order control system [1].

In this paper we use fractional-order PID (FrPID) controllers of type (1) for the analysis and control of a double integrator system in the presence of two nonlinearities (actuator saturation and output backlash). This study adopts the describing function method for the analysis of the fractional-order nonlinear control system, namely for the prediction of limit cycles. Several results are presented assessing the performance of the FrPID controllers in nonlinear systems.

Bearing these ideas in mind, the article is organized as follows. Section 2 reviews the fundamentals of fractional-order systems. Section 3 obtains the discretized form of the FrPID controller, while section 4 presents the basics of the describing function method of analysis. In section 5 we assess the performance of the FrPID controllers in the presence of two nonlinearities. Finally, section 6 draws the main conclusions.

2   Fundamentals of Fractional-Order Systems

The fractional-order systems deal with integrals and derivatives of arbitrary order (real or even complex order) (see [1]). There are different approaches to the definition of fractional-order integrals and derivatives, not being all equivalent. The Riemann-Liouville and the Grünwald-Letnikov definitions are the two most commonly used for this purpose. The Riemann-Liouville definition of the fractional-order derivative is ($\alpha > 0$):

$$_aD_t^\alpha f(t) = \frac{1}{\Gamma(n-\alpha)} \frac{d^n}{dt^n} \int_a^t \frac{f(\tau)}{(t-\tau)^{\alpha-n+1}} d\tau, \quad n-1 < \alpha < n \qquad (2)$$

where $\Gamma(x)$ is the Gamma function of x. By other hand, the Grünwald-Letnikov (GL) definition is formulated as ($\alpha \in \Re$):

$$_aD_t^\alpha f(t) = \lim_{h \to 0} \frac{1}{\Gamma(\alpha)} \sum_{k=0}^{\left[\frac{t-a}{h}\right]} (-1)^k \binom{\alpha}{k} f(t-kh) \qquad (3)$$

where h is the time increment and $[x]$ means the integer part of x. Note that the definitions (2) and (3) highlight the *global* character (*i.e.*, unlimited memory) of the fractional-order operators.

An alternative definition, which reveals useful for the analysis and control design of dynamic systems, is given through the Laplace transform (L) method. Considering vanishing initial conditions, this definition is given through the expected form:

$$L\left\{_aD_t^\alpha f(t)\right\} = s^\alpha F(s), \quad \alpha \in \Re \qquad (4)$$

where $F(s) = L\{f(t)\}$. Expression (4) is a direct generalization of the integer-order scheme with the multiplication of the signal transform $F(s)$ by the Laplace s-variable raised to a fractional value α. The Bode diagrams of amplitude and phase of (4) have a slope of 20α dB/dec and a constant phase of $\alpha\pi/2$ rad, respectively.

3 Discrete-Time Approximations of Fractional-Order Operators

The discrete-time implementation of the continuous $PI^\lambda D^\mu$-controller (1) can be obtained by adopting a generating function $s = w(z^{-1})$ [2, 3, 9], yielding:

$$C\left(z^{-1}\right) = K_p \left(1 + \frac{1}{T_i \left(w\left(z^{-1}\right)\right)^\lambda} + T_d \left(w\left(z^{-1}\right)\right)^\mu \right) \tag{5}$$

The discretization schemes most often used are the Al-Alaoui, Euler and Tustin operators. The Al-Alaoui scheme is a weighted interpolation of Tustin (1/4) and Euler (3/4) operators [7]. These $s \to z$ conversion schemes are special cases of the so-called T-integrator introduced by Smith [8]. This new type of integration formula is closely related to the mean value theorem. Thus, by adopting this operator, the discretization of s^α ($\alpha \in \Re$) is obtained by using the following generating function [9]:

$$\left(w\left(z^{-1}\right)\right)^\alpha = \left(\frac{1}{\delta T} \frac{1 - z^{-1}}{\gamma + (1-\gamma)z^{-1}} \right)^\alpha \tag{6}$$

where δ and γ are denoted the gain and phase tuning parameters, respectively. It is interesting to note that for $\delta = 1$ and varying γ from 0 to 2 in ratios of integers results in most of the useful classical discretization schemes. In fact, when $\delta = 1$ and $\gamma = \{1/2, 7/8, 1\}$, we obtain the Tustin, the Al-Alaoui and the Euler generating functions, respectively.

In order to get rational expressions to irrational function (6) (and, consequently, to the digital FrPID controller (5)) we can perform a continued fraction expansion (CFE) and the final approximation corresponds to a discrete rational transfer function (IIR filter) of the form [3, 9]:

$$D^\alpha(z) = \frac{Y(z)}{X(z)} = \left(\frac{1}{\delta T}\right)^\alpha \text{CFE} \left\{ \left(\frac{1 - z^{-1}}{\gamma + (1-\gamma)z^{-1}} \right)^\alpha \right\}_{m,n} = \left(\frac{1}{\delta T}\right)^\alpha \frac{P_m\left(z^{-1}, \alpha\right)}{Q_n\left(z^{-1}, \alpha\right)} \tag{7}$$

where m and n are the orders of the approximation, and P and Q are polynomials in the variable z^{-1} of degree m and n, respectively.

For example, by adopting a fractional-order derivative controller, D^α ($0 < \alpha < 1$), and using the Tustin operator as generating function ($\delta = 1$ and $\gamma = 1/2$ in (6)), we get the following IIR-type approximation for $m = n = 4$:

$$C\left(z^{-1}\right) = KD^\alpha \approx K\left(\frac{2}{T} \frac{1 - z^{-1}}{1 + z^{-1}}\right)^\alpha = K\left(\frac{2}{T}\right)^\alpha \frac{1 + p_1 z^{-1} + p_2 z^{-2} + p_3 z^{-3} + p_4 z^{-4}}{1 + q_1 z^{-1} + q_2 z^{-2} + q_3 z^{-3} + q_4 z^{-4}} \tag{8}$$

where K is the derivative gain constant and the coefficients (p_i, q_i), $i = 1, \ldots, 4$, are function of order α. A table with formulae for the calculation of the numerator and denominator coefficients of (8) can be found in [3]. Figure 1 shows the Bode diagrams of the approximation (8) for several values of order α and sampling period T (with $K = 1$).
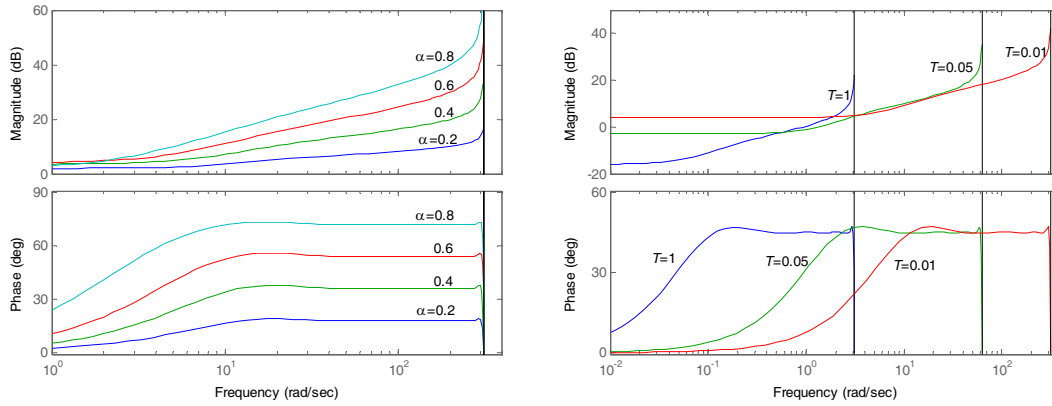
Figure 1: Bode diagrams for several values of order α (left) and sampling period T (right), with $K = 1$ and $m = n = 4$.

The Bode plots demonstrate the effectiveness of the approximations in fitting the ideal responses over a wide frequency range, in both magnitude and phase. It is also noted that the *width* of the approximation effectiveness' is not dependent on the sampling period, and that can be placed anywhere in the frequency domain by only varying the sampling period T.

4   Describing Function Analysis and Limit Cycle Prediction

In the analysis of nonlinear control systems by using the describing function (DF) method the nonlinearities of the system are grouped in only one block, $N(A,\omega)$, and the linear part grouped in another block, $L(s)$, as shown in Figure 2. Since the input is taken to be zero, the existence of (any) limit cycle is *predicted* if the following relationship holds:

$$N(A,\omega)L(j\omega) = -1 \tag{9}$$

or, in the more convenient form:

$$L(j\omega) = -\frac{1}{N(A,\omega)} \tag{10}$$

where $N(A,\omega)$ is the complex quantity given the phase-shift of the nonlinearity as function of frequency and amplitude. To graphically describe the occurrence of a possible limit cycle the Nyquist curve of $L(j\omega)$ is plotted together with $-1/N(A,\omega)$. Any intersection between these curves *predicts* a limit cycle and, consequently, their approximately amplitude A and frequency ω.
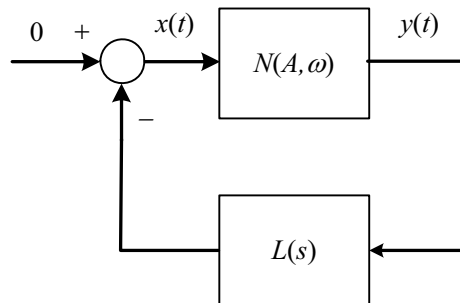

Figure 2: Nonlinear control system.

The describing function of the nonlinearity, $N(A,\omega)$, is determined by applying a sinusoid to the input of the nonlinear element, $x(t) = A\sin(\omega t)$, and then considering only the fundamental component of the output signal, $y(t)$. Thus, the DF (or the sinusoidal-input describing function) is defined as the complex ratio of the fundamental component of the output $y(t) = Y_1\sin(\omega t + \phi_1)$ and the input $x(t)$:

$$N(A,\omega) = \frac{Y_1}{A} e^{j\phi_1} \tag{11}$$

Such assumption of the DF is often valid since the higher-harmonics of $y(t)$ are usually of smaller amplitude than the amplitude of the fundamental component. Moreover, most systems are low-pass filters with the result that the higher-harmonics are further attenuated. For a meaningfulness use of the DF it is assumed that these conditions are fulfilled.

5 Performance of Fractional-Order Controllers in Nonlinear Systems

In order to study the performance of the fractional-order controllers in nonlinear control systems we adopt a simple prototype system with transfer function:

$$G(s) = \frac{k}{s^2} \tag{12}$$

with $k = 1$. Also, a fractional-order derivative controller, D^α, is used as fractional-order control algorithm for the case under study. The continuous transfer function of D^α is:

$$C(s) = Ks^\alpha \tag{13}$$

where K is the derivation constant.

The linear part of the nonlinear control system, $L(s)$, is then given by:

$$L(s) = C(s)G(s) = \frac{K}{s^{2-\alpha}} \tag{14}$$

The transfer function (14) is a fractional integral of order $\beta = 2-\alpha$, $0 < \alpha < 1$. The robustness of this system is illustrated through the root-locus depicted in Figure 3. In fact, when $1 < \beta < 2$, the root-locus follows the relation $\pi - \pi/\beta = \cos^{-1}\zeta$, where ζ is the damping ratio, independently of the gain K.
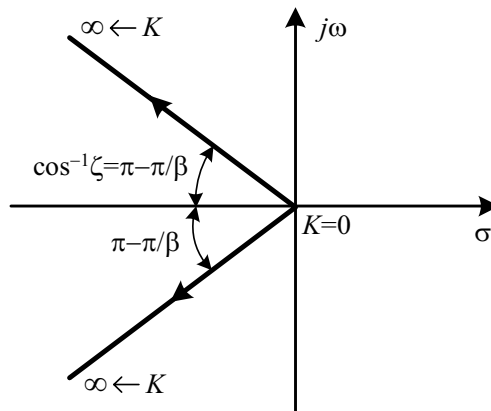

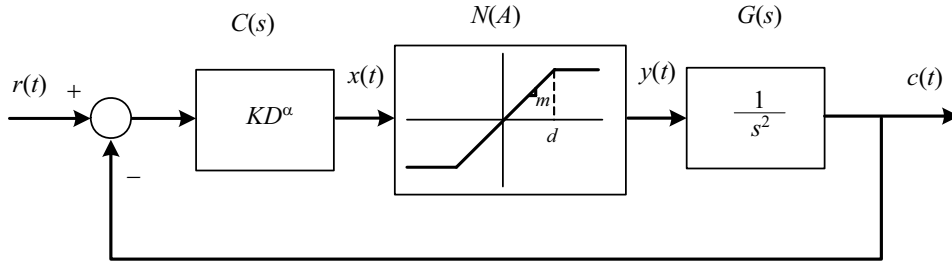Figure 3: Root-locus of linear part $L(s)$, $\beta = 2-\alpha$ ($0 < \alpha < 1$).

Figure 4: Nonlinear control system with saturation nonlinearity.

In a first phase, we consider the analysis of a nonlinear system with a saturation element at the actuator, as depicted in Figure 4.

The describing function of the saturation nonlinearity is computed as [10, 11]:

$$N(A) = \begin{cases} m, & 0 < A \le d \\ \dfrac{2m}{\pi}\left\{ \sin^{-1}\left(\dfrac{d}{A}\right) + \left(\dfrac{d}{A}\right)\sqrt{1 - \left(\dfrac{d}{A}\right)^2} \right\}, & A > d \end{cases} \tag{15}$$

Figures 5 and 6 illustrate the Nyquist diagrams of $L(s)$ and of $-1/N(A)$ as well the corresponding step responses when varying the gain K and the fractional-order α, respectively. The fractional-order controller D^α was implemented by using a 4th–order CFE approximation of type (8), with the Tustin operator, discretized at $T = 0.01$ s. For the saturation parameters we use $d = 1$ and $m = 1$. Note that the describing function of the saturation is a non-shifting phase (*i.e.*, Im[$N(A)$] = 0) and, consequently, the Nyquist plot of $-1/N(A)$ is placed over the negative real axis starting at point $(-1, 0)$. As can be seen from the Nyquist plots, the curves $L(s)$ and $-1/N(A)$ never intersect and, therefore, no limit cycle occurs. In this case, the system will be always stable. However, more can be said about the effect of the saturation on the control system's performance, by looking now at both graphs, the Nyquist plots and the step responses. The root-locus of this system (with the saturation removed) is depicted in Figure 3. We verify that, as the gain K is reduced, the locus shows that the roots move toward the origin of the s-plane while maintaining the same damping but different natural frequencies of oscillation. Figure 5 shows that the shape of the step responses remains almost unchanged (maintaining the same overshoot and natural frequency) independently of the system gain K, with exception for small values of K where the response becomes more oscillatory. This can be explained by noting that to large input signals corresponds a smaller equivalent gain of the saturation element. Therefore, as K increases, the (decreasing) gain of saturation will counteract with the larger input signal, maintaining the same location of the closed-loop poles in the root-locus. This results in the almost constant overshoot and natural frequency of the system. The variation of the order α of the fractional controller defines essentially the overshoot of the output response, as illustrated in Figure 6. However, for a strong derivative control action the system displays a large time delay. Figure 7 illustrates the influence of amplitude d of the saturation nonlinearity in the step responses for two values of order $\alpha = \{0.5, 0.8\}$, $K = 50$ and $m = 1$. As expected, the responses show the large influence of this parameter on system's performance, even for the case of nonlinear fractional-order systems.
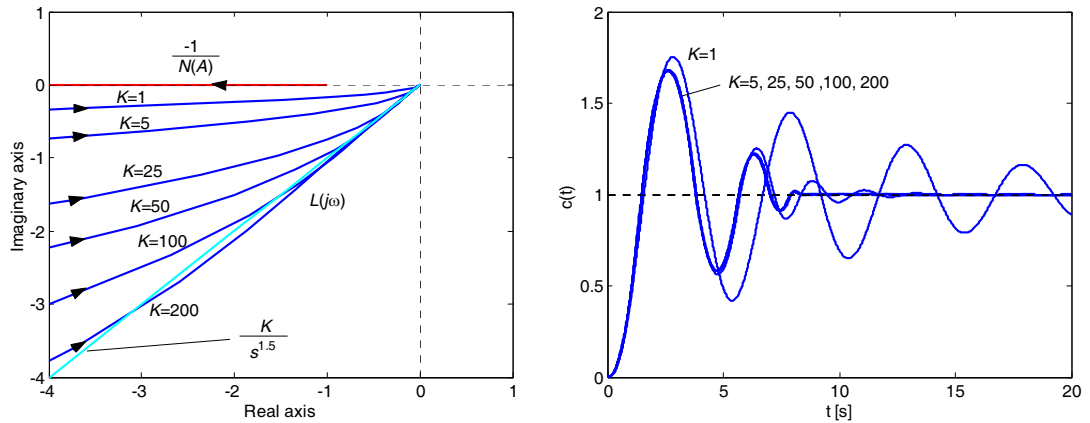
Figure 5: Nyquist diagrams (left) and step responses (right) for α = 0.5,
K = {1, 5, 25, 50, 100, 200}, m = 1, d = 1 and T = 0.01 s.
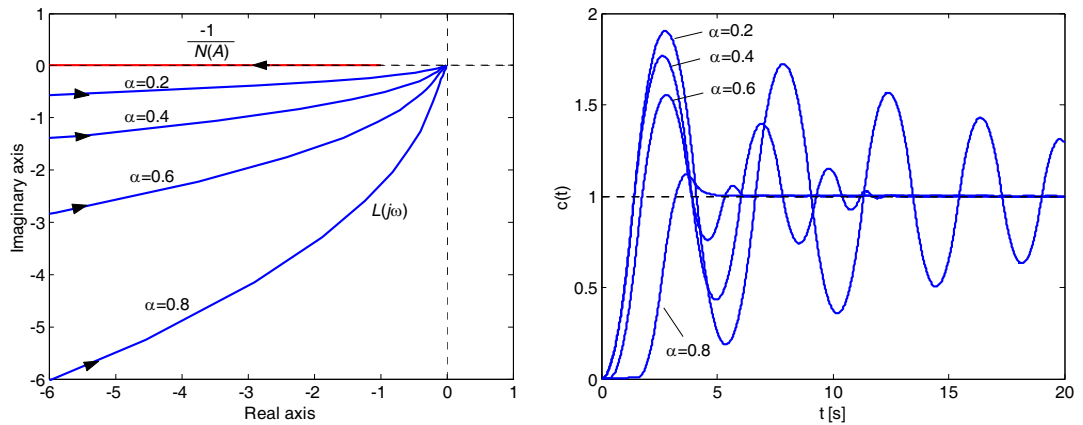

Figure 6: Nyquist diagrams (left) and step responses (right) for α = {0.2, 0.4, 0.6, 0.8},
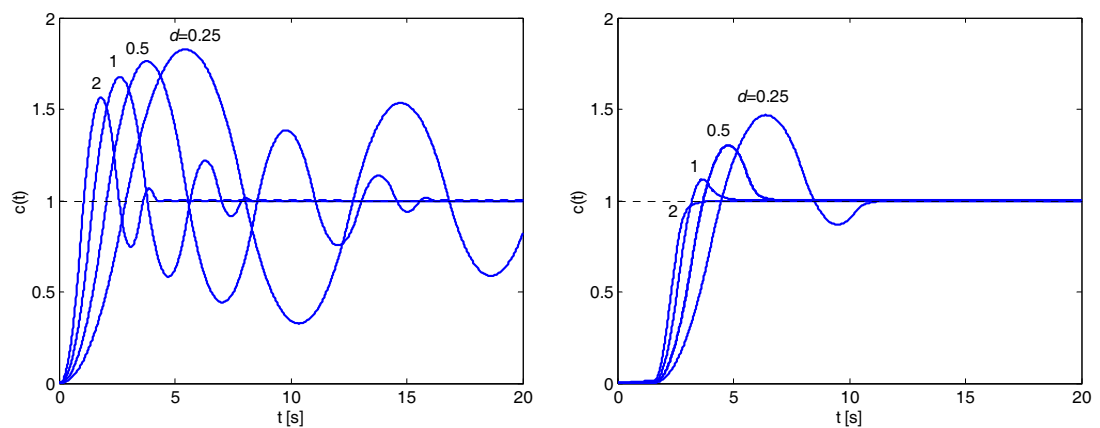K = 25, m = 1, d = 1 and T = 0.01 s.

Figure 7: Step responses with K = 50, m = 1, d = {0.25, 0.5, 1, 2} and T = 0.01 s for:
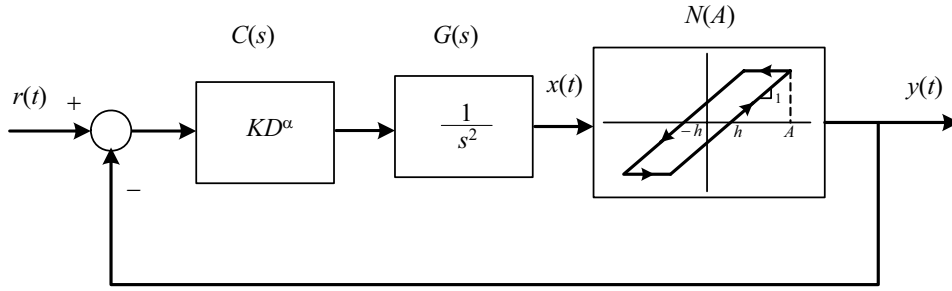left) α = 0.5 and right) α = 0.8.

Figure 8: Nonlinear control system with backlash nonlinearity.

Let us now consider a nonlinear control system with a fractional-order D^α controller, a double integrator prototype system $G(s)$ and a backlash nonlinearity $N(A)$ in the output, as illustrated in Figure 8. The linear part of the system, $L(s) = C(s)G(s)$, is identical to the one adopted in the previous example and is given by the transfer function (14).

The describing function of the backlash nonlinearity is defined by the following expression [11]:

$$N(A) = \frac{1}{2}\left[1 - N_s\left(\frac{A/h}{2 - A/h}\right)\right] - j\frac{4h(A-h)}{\pi A^2}, \quad A > h \tag{16}$$

where

$$N_s(x) = \frac{2}{\pi}\left[\sin^{-1}\frac{1}{x} + \frac{1}{x}\cos\left(\sin^{-1}\frac{1}{x}\right)\right] \tag{17}$$

Figures 9 and 10 illustrate the Nyquist diagrams of $L(s)$ and of $-1/N(A)$ as well the corresponding step responses for variation of the gain K and of fractional-order α, respectively. In this example, the fractional-order controller D^α is implemented through a 4th–order CFE approximation of type (8), with the Tustin operator, discretized at $T = 0.01$ s. In the backlash nonlinearity is adopted $h = 0.1$. Note that the describing function of the backlash is now phase shifting (with nonzero real and imaginary parts) and, consequently, the Nyquist plot of $-1/N(A)$ belongs to the third quadrant finishing into the point $(-1, 0)$, as shown by the Nyquist diagrams of Figures 9 and 10. In this case, the curves $L(s)$ and $-1/N(A)$ intersect always and, therefore, it is *always* predicted a limit cycle. We verify that the nature of this limit cycle is stable. Table 1 lists the approximated amplitudes and frequencies of the limit cycles, (A_0, ω_0), corresponding to Figures 9 and 10. Two methods are used for the limit cycle determination: *i*) describing function method and *ii*) time response simulation. As illustrated in Table 1, the calculated values of the limit cycles are very close in both cases showing the effectiveness of the describing function method in the prediction of limit cycles. This fact indicates the describing function method as useful tool in the analysis of nonlinear fractional-order systems.

In the first case (Figure 9), the step responses of the system exhibit an overshoot almost constant to large gain variations while varying the system natural frequency. These observations lead us to the conclusion that this system is somewhat robust against gain variations possessing an iso-damping property [12]. In the second case (Figure 10), we

verify that the order α establishes the response overshoot. These results are confirmed by the corresponding Nyquist plots.

Therefore, it is possible the system to yield a desired response by a suitable tuning of the gain K and order α. The approximations order $(m = n)$ is also one of the knob parameters that must be kept on consideration since it affects directly the results obtained.

In conclusion, the robustness of the fractional-order controllers is highlighted in the presence of nonlinearities. Nevertheless, from the perspective of controller performance, the tuning of K, α and of the order's approximation of the fractional-order operator require an optimization which will depend on the system dynamics. A systematic procedure for the controller design in the presence of nonlinear phenomena needs still further research.

A good starting point, as demonstrated in this study, is the application of the describing function method for the analysis of fractional-order nonlinear systems, which can be extended to the design of good generalized nonlinear controllers.
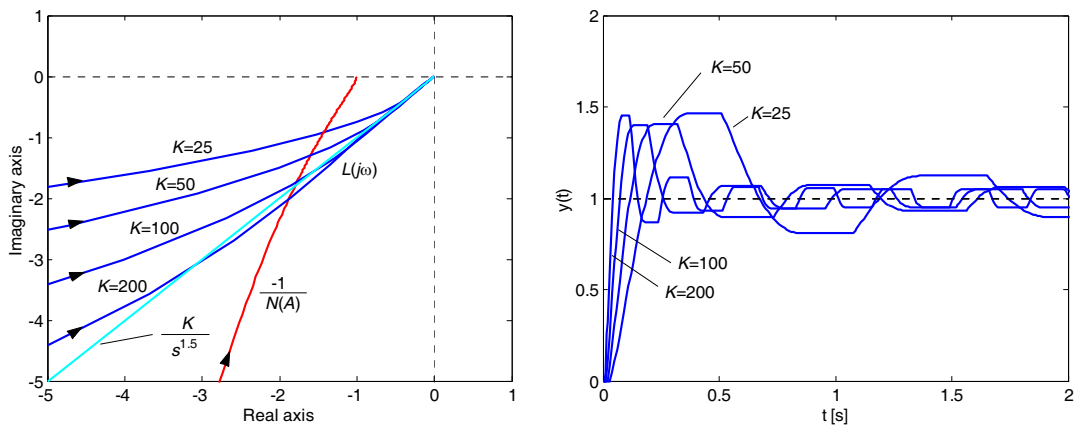
Figure 9: Nyquist diagrams (left) and step responses (right) for α = 0.5 and
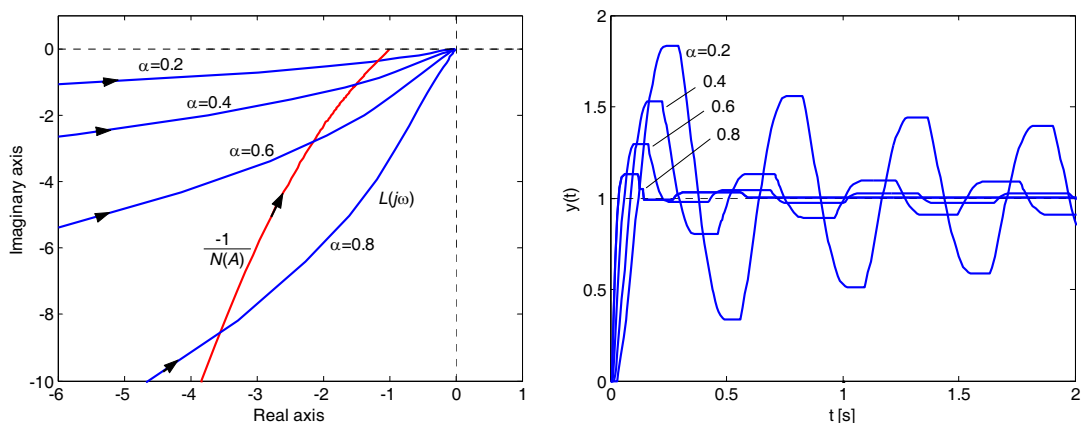$K = \{25, 50, 100, 200\}$, $h = 0.1$, $T = 0.01$ s.

Figure 10: Nyquist diagrams (left) and step responses (right) for α = {0.2, 0.4, 0.6, 0.8}
and $K = 100$, $h = 0.1$, $T = 0.01$ s.

Table 1: Amplitudes and frequencies of the limit cycles corresponding to Figure 9 (left) and Figure 10 (right).

Gain K	Predicted		Simulated		Order α	Predicted		Simulated	
	A_0	ω_0	A_0	ω_0		A_0	ω_0	A_0	ω_0
25	0.1973	5.4871	0.1915	5.3515	0.2	0.3781	11.2628	0.4534	11.5346
50	0.1670	7.6237	0.1626	7.4290	0.4	0.1832	11.4531	0.1891	11.7447
100	0.1494	10.9515	0.1492	11.0537	0.6	0.1294	9.9578	0.1266	9.6258
200	0.1421	16.9224	0.1512	18.8640	0.8	0.1093	6.5282	0.1057	4.7600

6 Conclusions

In this paper we have assessed the performance of fractional-order controllers in the presence of two nonlinear elements: actuator saturation and output backlash. We have also found the describing function method of analysis a very useful tool for the study of fractional-order nonlinear systems. For a double integrator prototype system the control algorithms based on the fractional-order concepts are simple to implement and reveal good robustness. However, a more systematic procedure for the controller design in the presence of nonlinear phenomena needs still further research.

References

[1] I. Podlubny. *Fractional Differential Equations*. Academic Press, San Diego, 1999.

[2] J. A. Tenreiro Machado. Discrete-Time Fractional-Order Controllers. *FCAA Fractional Calculus & Applied Analysis*, 4(1):47−66, 2001.

[3] B. M. Vinagre, Y. Q. Chen, I. Petras. Two direct Tustin discretizations methods for fractional-order differentiator/integrator. *Journal of the Franklin Institute*, 340:349−362, 2003.

[4] S. Manabe. The system design by the use of a model consisting of a saturation and non-integer integrals. *ETJ of Japan*, 8(3/4):147−150, 1963.

[5] S. Manabe. Early development of fractional order control. *Proc. of the 19th Biennial Conference on Mechanical Vibration and Noise (VIB'03)*, Chicago, USA, September 2−6, 2003.

[6] P. Lanusse, A. Oustaloup and J. Sabatier. Step-by-step presentation of a 3rd generation CRONE controller design with anti-windup system. *Proc. of the Fifth EUROMECH Nonlinear Dynamics Conference (ENOC'05)*, Eindhoven, The Netherlands, August 7−12, 2005.

[7] M. A. Al-Alaoui. Novel digital integrator and differentiator. *Electronics Letters*, 29(4):376−378, 1993.

[8] J. M. Smith. *Mathematical Modeling and Digital Simulation for Engineers and Scientists*. Wiley & Sons, 2nd edition, New York, 1987.

[9] Ramiro S. Barbosa, J. A. Tenreiro Machado and Manuel F. Silva. Time domain design of fractional differintegrators using least-squares. *Signal Processing*, Elsevier, 2006.

[10] J. E. Slotine and W. Li. *Applied Nonlinear Control*. Prentice-Hall, New Jersey, 1991.

[11] C. Phillips and R. Harbor. *Feedback Control Systems*. Prentice-Hall, New Jersey, 1996.

[12] Ramiro S. Barbosa, J. A. Tenreiro Machado and Isabel M. Ferreira. Tuning of PID controllers based on Bode's ideal transfer function. *Nonlinear Dynamics*, 38(1−4):305−321, 2004.